

---

# Advanced Brain Tumour Segmentation from MRI Images

---

Kavitha Angamuthu Rajasekaran and  
Chellamuthu Chinna Gounder

Additional information is available at the end of the chapter

<http://dx.doi.org/10.5772/intechopen.71416>

---

## Abstract

Magnetic resonance imaging (MRI) is widely used medical technology for diagnosis of various tissue abnormalities, detection of tumors. The active development in the computerized medical image segmentation has played a vital role in scientific research. This helps the doctors to take necessary treatment in an easy manner with fast decision making. Brain tumor segmentation is a hot point in the research field of Information technology with biomedical engineering. The brain tumor segmentation is motivated by assessing tumor growth, treatment responses, computer-based surgery, treatment of radiation therapy, and developing tumor growth models. Therefore, computer-aided diagnostic system is meaningful in medical treatments to reducing the workload of doctors and giving the accurate results. This chapter explains the causes, awareness of brain tumor segmentation and its classification, MRI scanning process and its operation, brain tumor classifications, and different segmentation methodologies.

**Keywords:** magnetic resonance imaging, segmentation, classification, tumor, diagnostic system

---

## 1. Basics of medical research

Digital image processing is a multidisciplinary area used in medical sciences, microscopy, astronomy, computer vision, geology, and many other fields. Medical imaging is one of the most important aspects of scientific and medical research. It provides computerized medical-image segmentation and computer-aided design. Particularly, these enhancements in medical imaging lead to the improved planning and accuracy of surgical procedures using human-machine intervention. This brings the therapeutic plan and the development of imaging instruments to provide some of the most effective diagnostic tools in the medical field. Recently, many medical instruments have been developed to produce sectional views of the human anatomy. The two major non-invasive techniques used for imaging the human body

---

are computed tomography (CT) and magnetic resonance imaging (MRI). The MRI is used as a medical diagnostic tool for studying the human anatomy and is based on the principles of nuclear magnetic resonance (NMR), to provide information about the properties of materials. The NMR was developed by Bloch and Purcell in the 1940s [1, 2]. In the year 1970, Paul Lautenberg, Ray Damadian, and Peter Mansfield began to use the principles of NMR in MRI as an imaging modality for the head, spine, and body. MRI produces images of high spatial resolution with good soft tissue contrast that has made it useful for the detection of diseases. In x, Paul Lauterbur and Peter Mansfield were awarded the Nobel Prize in Physiology or Medicine for their simultaneous pioneering research applying MRI to the human body [3].

### 1.1. Motivation for brain tumor segmentation

Brain tumor segmentation is one of the most important and difficult tasks in many medical-image applications because it usually involves a huge amount of data. Artifacts due to patient's motion, limited acquisition time, and soft tissue boundaries are usually not well defined. There are large class of tumor types which have variety of shapes and sizes. They may appear indifferent sizes and types with different image intensities. Some of them may also affect the surrounding structures that change the image intensities around the tumor.

Moreover, the World Health Organization (WHO) states that around 400,000 people in the world are affected with the brain tumor and 120,000 people have died in the previous year [4–7]. Before the treatment of chemotherapy, radiotherapy, or brain surgeries, there is a need for medical practitioners to confirm the boundaries and regions of the brain tumor and determine where exactly it is located and the exact affected area. For reviewing the adverse effects of the cancer, the tool can be automatic or semi-automatic for brain tumor segmentation can helps and also acts as a pre-requisite stage for doctors to identify the brain tumor before performing surgeries.

### 1.2. Magnetic resonance imaging (MRI)

The MRI is a diagnostic tool used for analyzing and studying the human anatomy. Huang [8], Zhan et al. [9], and Yang et al. [10] explained the medical images acquired in various bands of the electromagnetic spectrum. The wide variety of sensors used for the acquisition of images and the physics behind them, make each modality suitable for a specific purpose.

In MRI, the pictures are produced using a magnetic field, which is approximately 10,000 times stronger than the earth's magnetic field (Armstrong [11], Stark [6], and Steen [7]). The MRI produces more detailed images than other techniques, such as CT or ultrasound. The MRI also provides maps of anatomical structures with a high soft-tissue contrast. Basically, the magnetic resonance of hydrogen ( $^1\text{H}$ ) nuclei in water and lipid is measured by an MRI scanner. As the signal values are 12-bit coded, 4096 shades can be represented by a pixel [11]. The MRI scanners require a magnetic field and it is available at 1.5 or 3 T. In comparison with the earth's magnetic field ( $\sim 50 \mu\text{T}$ ) the magnetic field of a 3 T MRI scanner is approximately 60,000 times the earth field. The patient is placed in a strong magnetic field, which causes the protons in the water molecules of the body to align either in a parallel or anti-parallel orientation with the magnetic field. A radiofrequency pulse is introduced, causing the spinning protons to move

out of the alignment. When the pulse is stopped, the protons realign and emit radio frequency energy signal that is localized by the magnetic fields and are spatially varied and rapidly turned on and off. A radio antenna within the scanner detects the signal and creates the image. Terms used in MRI are shown in **Table 1**.

MR-based imaging techniques are used to characterize the brain tumor according to their anatomy and physiology. Clinicians, particularly are interested in determining tumor location, extent, amount of necrosis, vascular supply, and associated edema. There are different imaging techniques that are useful in providing a relevant differential diagnosis. The various techniques used today for imaging brain tumor are contrast agents, fat suppression, MR angiography, functional MRI, diffusion weighted imaging (DWI), MR spectroscopy, and fast fluid-attenuated inversion-recovery (FLAIR). Different methods of imaging are applied in the clinical environment according to tumor type and diagnostic requirements. The methods used in the diagnosis work are described in detail [8, 12].

The contrast agents technique delivers an excellent soft-tissue contrast. Sometimes there is a need to administer exogenous contrast usually an intravenous injection of some paramagnetic agent, most commonly Gd-DTPA. The effect of this agent is to shorten the relaxation time of local spins causing a decrease in signal on T2-weighted images and an increase on T1-weighted images. The MRI brain image before and after contrast enhancement is shown in **Figure 1**.

The increased vascularity of tumors produces a preferential uptake of contrast agent and it can be used to better observe the tumors from the surrounding normal tissue. If MRI scans are repeatedly acquired following the contrast injection, the dynamic nature of contrast uptake can be examined, which may improve the differentiation of benign and malignant disease.

MR angiography is one of the biggest growth areas of MRI. In normal circumstances, the flow effects can cause unwanted artifacts. But, in MRA these phenomena are used advantageously to permit the non-invasive imaging of the vascular tree. Techniques can be generally divided into “white” or “black” blood methods depending on whether moving spins appear brighter

Term	Description
T1	The time needed for the protons in the tissue to return to their original state of magnetization
T2	The time required for the protons perturbed into coherent oscillation by the radiofrequency pulse to loosen this coherence
TR	Repetition time: the time between successive applications of radiofrequency pulse sequences
TE	Echo time: the delay before the radiofrequency energy radiated by the tissue in question is measured
T1-weighted image	Short TR, short TE. Provides better anatomic detail
T2-weighted image	Long TR, short TE. More sensitive to water content and as a result, more sensitive to pathology
FLAIR image	Long TR, short TE. Improved contrast between lesions and cerebrospinal fluid

**Table 1.** Summaries of terms used in MRI.

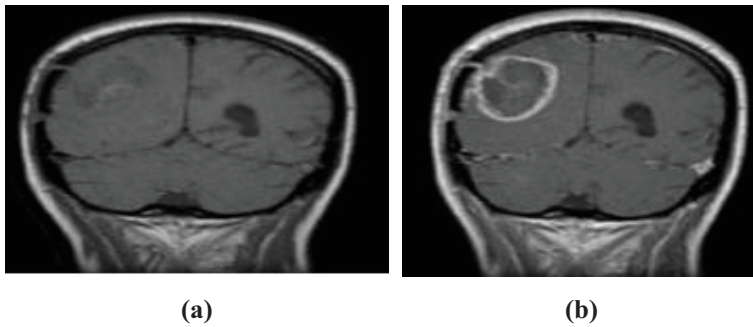


**Figure 1.** MRI image contrast enhancement. (a) Before (b) after.

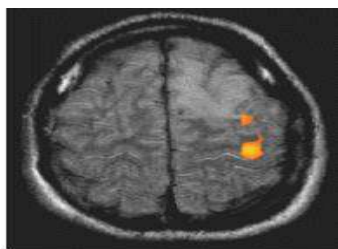
or darker than the stationary tissue. In high-velocity signal loss, the blood that has moved in-between  $90^\circ$  and  $180^\circ$  pulses will not produce a signal and will appear dark. If a short TR is used, the spins in the imaging slice become quickly saturated and “fresh” spins flowing into this slice have their full magnetization available to emit a high signal. This technique works the best way over thin sections when blood flow is perpendicular to the imaging plane. Although current clinical agents are extracellular, they quickly distribute into the extra vascular space and the accurate timing of imaging sequence following the contrast injection can provide excellent results. Good timing of arterial bolus with the center of k-space acquisition is crucial to avoid artifacts. This can be achieved by using a small “test bolus” or by monitoring the contrast flow using rapid 2D images before initiating the real imaging sequence. The angiography provided by MRI imaging is shown in **Figure 2**.

Functional MRI is a technique for examining the brain activation, which unlike PET, is non-invasive with relatively high spatial resolution. The most common method utilizes a technique called blood oxygen level dependent contrast. This is an example of endogenous contrast, making use of the inherent signal differences in blood oxygenation content. In the normal resting state, a high concentration of deoxyhemoglobin attenuates the MRI signal due to its paramagnetic nature. However, the neuronal activity, in response to some task or stimulus, creates a local demand for the oxygen supply, which increases the fraction of oxy hemoglobin causing a signal increase on T2 or T2\*-weighted images. In a typical experiment, the patient is subjected to a series of rest and task intervals, during which MRI images are repeatedly acquired. The signal changes during the course of time are then examined on a pixel-by-pixel basis to test how well they correlate with the known stimulus pattern. The pixels that demonstrate a statistically significant correlation are highlighted in color and overlaid onto a gray-scale MRI image to create an activation map of the brain. The location and extent of activation is linked to the type of stimulus. Thus, a simple thumb-finger movement task will produce activation in the primary motor cortex. The functional study and activation map of MRI is shown in **Figure 3**.

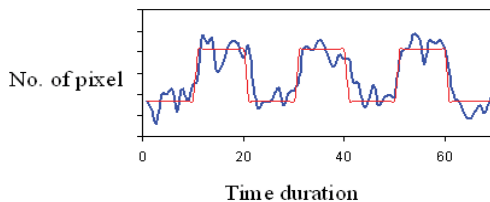
Diffusion-weighted imaging is an MRI technique, in which contrast within the image is based on the movement of the water molecules. The diffusion refers to the random motion of the molecules along a concentration gradient. The diffusion-weighted MRI is another example of



Figure 2. MRI angiography (Courtesy: Siemens.com).



(a)



(b)

Figure 3. Functional study of MRI. (a) MRI image (b) activation map of the MRI image.

endogenous contrast, using the motion of spins to produce signal changes. The most common method employs the Stejskal-Tanner bipolar gradient scheme. The gradients with equal amplitude, but opposite polarity, are applied over a given interval. The stationary tissue is dephased and rephased equally, whereas the spins which have moved during the interval suffer a net dephasing and signal loss. By using gradients of sufficiently high amplitude, the sequence is made sensitive to the motion at the microscopic level. The signal attenuation depends on the degree of diffusion, the strength, and the timing of the gradients. By acquiring the images with different values of  $b$  factor, a value for the apparent diffusion coefficient can be calculated. The

experiment is performed using diffusion gradients in any direction. However, to obtain a complete three-dimensional description of the diffusion, a tensor is calculated based on a new gradient image and combinations of gradient pairs. This is able to discern anisotropy due to preferential diffusion along the structures or fibers. The white matter tracts in a normal MRI brain image are shown in **Figure 4**.

MRI spectroscopy is a technique for displaying the metabolic information from an image. It relies on the inherent differences in the resonant frequency. The MRI signal is measured and a spectrum is displayed. By using a standard reference, the chemical species of each peak are determined. For proton MRI signal, the reference compound is tetramethylsilane. All the chemical shifts are expressed as the frequency differences from this compound giving a field-independent part per million scales. In this standard, the water has characteristic peak value of 4.7 ppm. Most methods use the intersection of three slice-select RF pulses to excite a volume of interest called a voxel.

The multiple voxels can be acquired by using phase encoding in each of the desired dimensions. This technique, called chemical shift imaging, is useful in isolating individual peaks and displaying the integrated area as a color scale to produce a metabolic map. The spectrum when acquired from a normal healthy brain tissue displays the characteristic peak signal defined as NAA; it provides images with excellent soft-tissue contrast. If a spectrum is taken from a slightly enlarged, but otherwise normal looking, part of the medulla, it does not show any enhancement with gadolinium. In this case, the NAA (*N-acetyl-aspartate*) peak is absent indicating the loss of viable tissue, and the choline peak is elevated indicating the high cell proliferation in tumors. The single voxel proton MRI of brain in normal and malignant tissue is shown in **Figure 5**.

The MRI images are dependent upon the absorption of radio waves by the hydrogen nuclei,  $^1\text{H}$  which has an intrinsic nuclear spin in sufficient quantities to enable the production of a useful image of the human body. Many of the protons within the human body are found in the nuclei of water. The generation of MRI images is a result of the sophisticated interaction

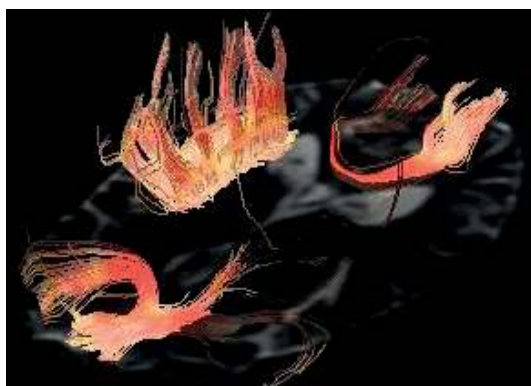


**Figure 4.** White matter tracks in a normal MRI brain image.

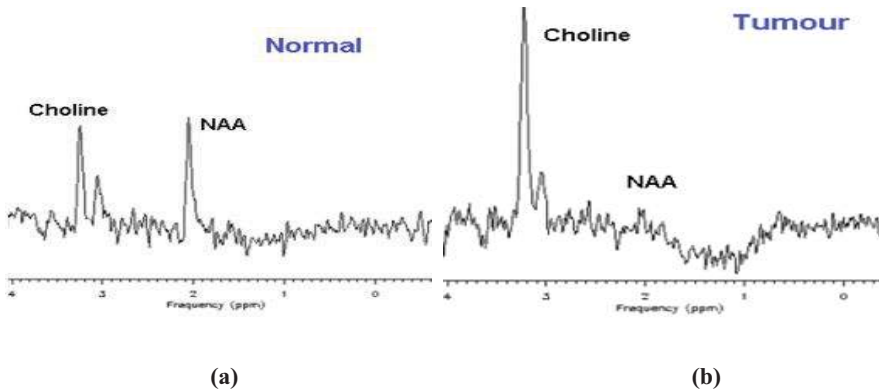


**Figure 5.** Single voxel proton MRI brain in normal and malignant tissue. (a) Normal (b) With tumour.

between the electronic components, radiofrequency generators, coils, and gradient that interface with a computer for communication between the different electronics. The magnet, gradient coils, and RF coils present in the MRI scanner are the basic parts that help to form an image. The schematic diagram of MRI scanner and the basic parts of the MRI scanner are shown in **Figure 6** [9, 13].

The magnet is used to form the “external” magnetic field in which the patient or object is placed. Three types of magnets can be used in MR imaging: permanent, resistive, and superconducting. The superconducting magnets are the most commonly used in the recent MRI scanners. The superconducting magnets with field strength 1.5–3.0 T range offer good image contrast due to the energy exchange between the protons and their environments.

The hydrogen proton is the primary nucleus used for MRI because it produces the strongest signal. Proton in the absence of an external magnetic field may be oriented along any direction. In the absence of an external magnetic field, the net magnetization vector will be zero. When placed in a strong external magnetic field the magnetic moments of the proton orient themselves along the magnetic flux lines. The magnetic moments of the protons align along the direction of actual magnetic field  $B_0$ . The equilibrium value of the magnitude of proton magnetization  $M_0$  in the presence of magnetic field is given in Eq (1).

$$M_0 = \frac{N\gamma^2 h^2 I(I + 1) B_0}{3kT_s} \quad (1)$$

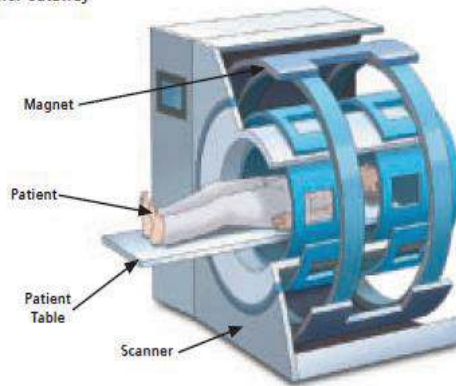
where  $B_0$  is the static magnetic field,  $N$  is the number of proton spins per unit volume,  $\gamma$  is the gyro magnetic ratio, a constant unique for each nucleus,  $h$  is the Planck’s constant,  $I$  is the proton spin,  $T_s$  is the absolute sample temperature in Kelvin, and  $k$  is the Boltzmann’s constant.

Thus, the magnetization  $M_0$  is proportional to the external magnetic field  $B_0$ . The magnetic moments exhibit the property of precessing around the field  $B_0$ . The Larmor frequency in MRI refers to the rate of precession of spin under the influence of magnetic moment of the proton around the external magnetic field. The precession of Larmor frequency  $f_L$  is given in Eq (2).



(a)

MRI Scanner Cutaway



(b)

**Figure 6.** View of MRI scanner and the basic parts of MRI scanner. (a) The schematic diagram of MRI scanner (b) basic parts of the MRI scanner.

$$f_L = \frac{\gamma B_0}{2\pi} \quad (2)$$

For the proton,  $\frac{\gamma}{2\pi}$  is equal to 42.58 MHz/Tesla. The Larmor frequency will be in the radio frequency region (40–50 MHz).

To obtain an MRI signal, the radio frequency (RF) pulses are applied at the Larmor frequency  $f_L$  perpendicular to the main magnetic field  $B_0$  disturbing the magnetic moments of the protons



from their equilibrium position. The protons are aligned along the static magnetic field. This alignment is disturbed by a  $90^\circ$  RF pulse and the total displacement is proportional to the RF-pulse energy and also the Larmor frequency. If the energy of the RF pulse is sufficient to tip the magnetization vector ( $M$ ) by  $90^\circ$ , then it is tipped into the transverse plane. The magnetization vector continues to spinning process about  $B_0$  in the transverse plane. The time-varying magnetization induces flux changes, which are detected in the RF coil. The relaxation constants are the important parameters of MRI. The MRI slice data are generated using an X-ray source that rotates around the object. The earliest sensors were scintillation detectors, with photo multiplier tubes excited by cesium iodide crystals. Cesium iodide was replaced during the 1980s by ion chambers containing high pressure xenon gas [14]. These systems were, in turn, replaced by scintillation systems based on the photo diodes, instead of photo multipliers. Many data scans are progressively taken, as the object is gradually passed through the gantry. The typical MRI system with the schematic diagram of MRI equipment mainly consists of five parts: the main magnet, gradient systems, RF system, computer systems, and other auxiliary equipment as shown in **Figure 7**.

The direction selection for MRI slices and MRI scan protocol [15, 16] for brain tumor patients are shown in **Figure 8** and **Table 2**.

In the MRI scanner, a section of the slice perpendicular to the z-axis is called axial plane. The plane that divides the brain into left and right parts is known as sagittal or median plane. The vertical plane that divides the brain into posterior and anterior parts is known as coronal or frontal plane. The MRI brain image in different planes is shown in the **Figure 9**.

MRI pixel representation mainly in order to increase the contrast between pathology and healthy tissue, enhancement agents such as gadolinium (Gd) may be used (Kim et al. 2013). The Gd has a large magnetic moment, which triggers fluctuations in the local magnetic field near the Larmor frequency. The MRI images are grids of pixels with 512 rows and 512

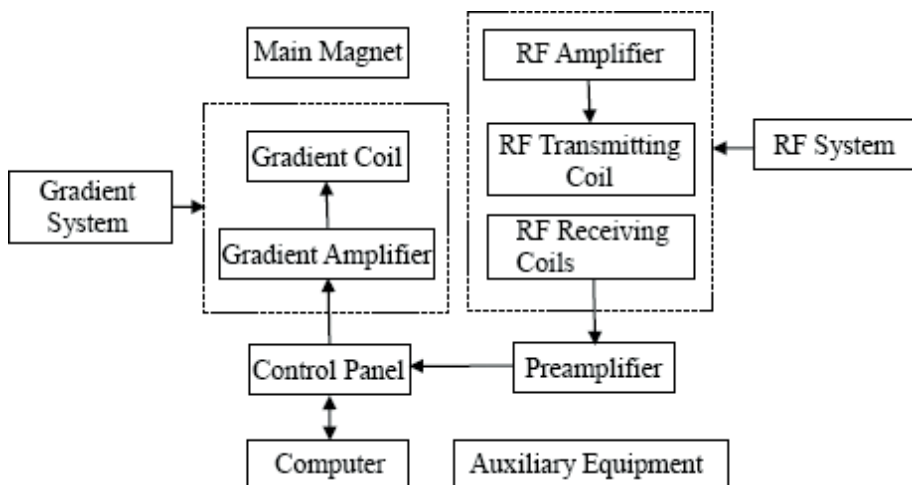


**Figure 7.** The schematic diagram of MRI equipment and MRI scan process.

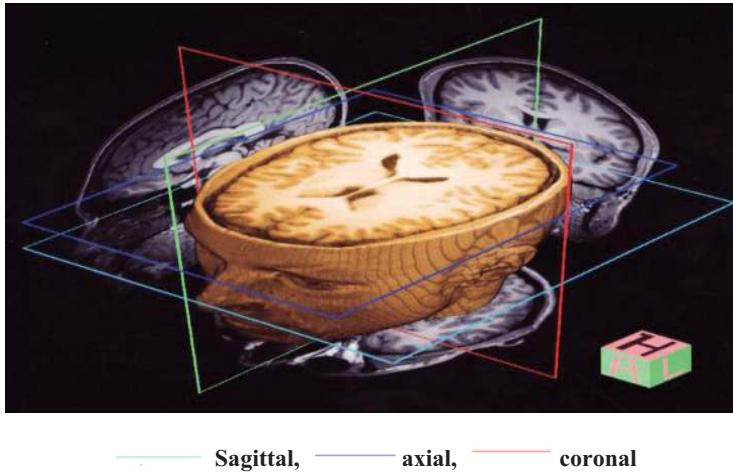


Figure 8. The direction selection in MRI slices.

Anatomical plane	Weighting	Contrast	Slice thickness/spacing between slices (in mm)
Sagittal	T1-Weighted	—	5/6
Axial	T1-Weighted	—	4/4
Axial	T2-weighted	—	5/6
Axial	T2-weightedFLAIR	—	5/6
Axial	T1-Weighted	Gadolinium	4/4
coronal	T1-Weighted	Gadolinium	4/4
Sagittal	T1-Weighted	Gadolinium	5/6

Table 2. MRI scan protocol for brain tumor patients [15].

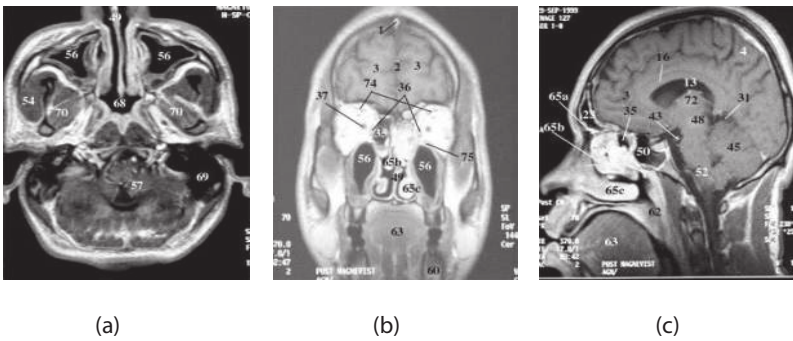


Figure 9. MRI brain image in different planes. (a) Axial (b) Coronal (c) Sagittal.

columns. Every pixel of an MRI image corresponds to a voxel, a volume element, whose value represents the tissue and MRI signal. The volume of a voxel depends on the MRI scan parameters like slice thickness and pixel spacing. The MRI images are usually delivered in DICOM format. Besides the brain image, the DICOM-files contain information about the scan and the patient. Normally, an MRI scan acquires more than one slice, which leads to an image sequence with 5.5 mm spacing between the slices [17]. The sequence of MRI for 256 slices is shown in **Figure 10** with 5.5 mm spacing between the slices.

In this thesis, the segmentation algorithm is applied to the MRI brain images with tumors. In order to understand the clinically important characteristics of the tumor tissues, the anatomy of brain is considered in the next section.

### 1.3. Anatomy of the brain classification of brain tumor

World Health Organization (WHO) classifies the brain tumors as: astrocytoma, low grade astrocytoma (grades I and II), high grade astrocytoma (grades III and IV), ganglioglioma, oligodendroglioma, ependymoma, and medulloblastoma.

The higher the grade, the more malignant is the tumor. The tumor grading helps the doctor, patient, and caregivers/family members to understand the patient's condition [18]. It also helps the doctor to plan treatment and predict outcome.

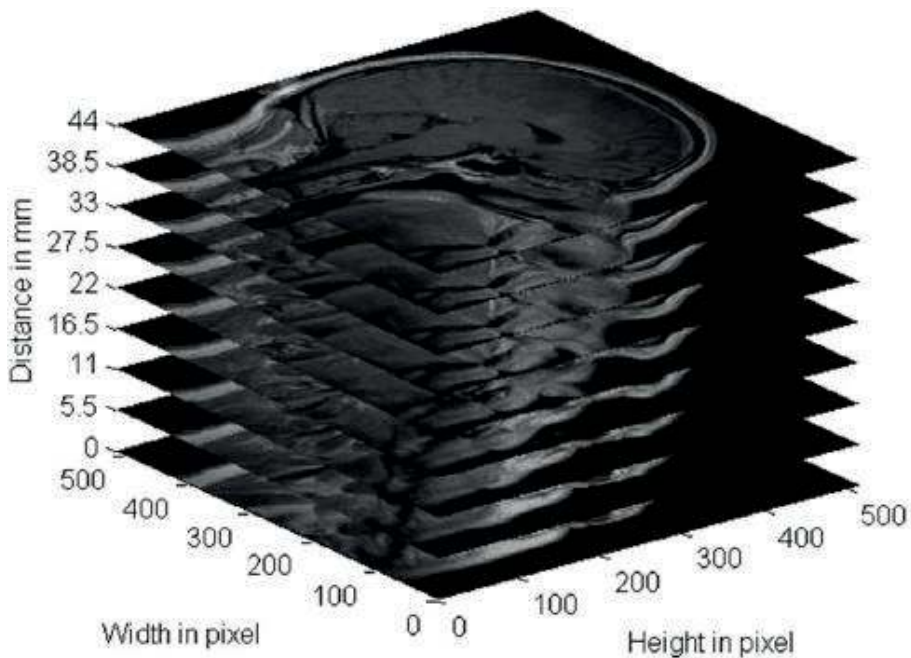


**Figure 10.** MRI sequence with 5.5 mm spacing between slices.

Grade-I is indicative of the least malignant tumors and is usually associated with long-term survival. These tumors grow slowly and have an almost normal appearance when viewed through a microscope. Only surgery may be required as an effective treatment for this grade tumor [19]. Pilocytic astrocytoma, craniopharyngioma, and other tumors of neurons such as gangliocytoma and ganglioglioma are the examples of grade I tumors.

Grade II tumors are slow-growing and look slightly abnormal under a microscope. Some can spread into nearby normal tissue and recur sometimes as a higher grade tumor.

Grade III tumors are, by definition, malignant although there is not always a big difference between grade II and grade III tumors. The cells of a grade III tumor are actively reproducing abnormal cells, which grow into nearby normal brain tissue. These tumors tend to recur often as a grade IV.

Grade IV are the most malignant tumors. They can have a bizarre appearance when viewed under the microscope, and easily grow into nearby normal brain tissue. These tumors form new blood vessels so that they can maintain their rapid growth. They also have areas of dead cells in their centers. The glioblastoma multiform is the most common example of a grade IV tumor. A sample of astrocytoma is (cite [20]) shown in **Figure 11**.

There are three classifications of tumors based on their location: local tumors, regional tumors, and distant tumors. The local tumors are confined to one hemisphere in one part of the brain, meninges, and ventricular system. The regional tumor crosses the midline or tentorium and invades bone, blood vessel, nerves, and spinal cord [16]. The distant tumors extend to the nasal cavity, nasal pharynx, and posterior pharynx.

Classification of tumors based on their radiological appearance includes non-enhanced tumors, full-enhanced tumors without edema, full-enhanced tumors with edema, and ring-enhanced tumors. Classification of tumors based on their alter-At ions consists of small deforming tumors (SD) and large deforming tumors (LD).

Brain tumor is diagnosed when a brain tumor is suspected; a doctor can carry out a number of tests to reach a diagnosis. These tests will help the doctor to determine the kind of tumor in the brain.

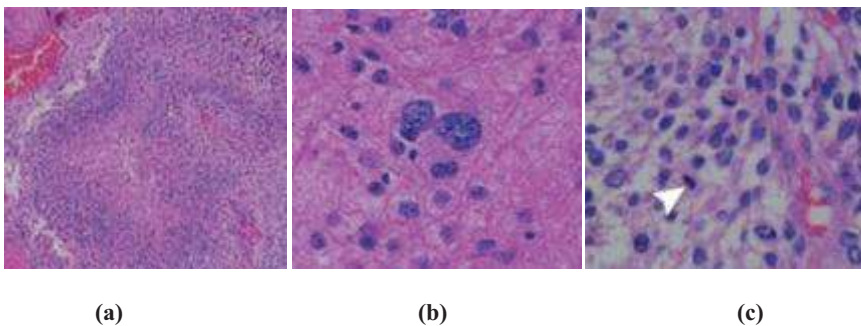


**Figure 11.** Sample of astrocytoma. (a)Astrocytoma IV (b) Astrocytoma II (c)Astrocytoma III.

Some of the tests are performed first to diagnose the tumor and the results are used later to monitor the progress to determine whether the tumor has disappeared, is shrinking, remaining the same, or has changed in some way. Like many other medical conditions, the follow-up care for a brain tumor might go on for years.

The brain tumor diagnosis [16] is executed based on the Neurological Exam, Types of brain scans, X-rays, Laboratory test, DNA profiling, Biopsy procedure, and Tumor grading and staging.

A neurological exam includes a series of tests and procedures used to assess a person's nerves, senses, muscle strength, reflexes, balance, and mental state. The purpose of a neurological exam is to help the doctor determine the cause of the symptoms that brought the patient into the clinic in the first place.

MRI scans generate images of the brain for the purpose of diagnosing the tumor. The most common scans for diagnosis and follow-up are: MRI, CT, FMRI, dynamic MRI, angiography and MRI angiography MRS, positron emission tomography, single photon emission computerized tomography, and magneto encephalography.

The genetic profiling, or DNA profiling, is a lab test used to determine the specific features of patient DNA. It is a relatively new procedure that can give the doctor detailed information about the tumor. This information is used to develop a more specialized course of treatment, which may significantly increase the odds of success. A biopsy is a surgical procedure, in which a small amount of tumor tissue is removed and sent to a lab for evaluation. The purpose of a biopsy is to establish whether an image is cancerous or not. The biopsy can be performed as part of the surgery to remove a tumor, or as a separate procedure. In either case, the surgeon removes a small amount of tumor tissue and sends it to a lab for a pathologist to review. Three types of biopsy are often performed in patients with brain tumors. These include needle biopsy, stereotactic biopsy, and open biopsy. If the results of patient's biopsy are not normal, the patient goes back to the doctor for further tests and advice.

#### **1.4. Brain tumor segmentation**

A lot of research has been carried out in the area of segmentation. Various segmentation techniques are addressed in this survey. The content of this survey comprises three important contributions: fuzzy C-means (FCM), region growing (RG), and genetic-based methods. The aim is to study and identify of the suitable segmentation for MRI images. This above said aim is to grasp the characteristics of tumors in the patients, automatically segment the tumor, and assist the doctors in assessing the effects of treatment with clinical pathology analysis and improving the therapeutic treatment in the next pathological periods.

##### *1.4.1. Image segmentation using fuzzy C-means (FCM) method*

The fuzzy C-means method description and some of the recent researches for segmentation based on genetic methodologies are as follows:

The FCM is the most widespread clustering algorithm [21, 22], but it is more sensitive to initial cluster centers and easy to fall into the local minimum value, so that the global optimal

solution cannot be obtained due to the local search hill-climbing method. The traditional FCM for image segmentation directly performs the clustering for pixel sample sets with an obvious disadvantage of computational complexity. So, it is very important to choose better initial cluster centers. If we choose better initial cluster centers, algorithm can converge to the real cluster centers quickly. The FCM algorithm is successfully applied in many real world problems such as astronomy, geology, medical imaging, target recognition, and image segmentation. FCM segmentation method has considerable benefits, because it could retain much more information from the original image than hard segmentation method [23]. The FCM algorithm is composed of the following steps:

1. Initialize

$$U = [u_{ij}] \text{ matrix, } U^{(0)} \quad (3)$$

2. At k-step: calculate the centers vectors  $c^{(k)} = [c_j]$  with  $U^{(k)}$

$$c_{ij} = \frac{\sum_{i=1}^N u_{ij}^m x_j}{\sum_{i=1}^N u_{ij}^m} \quad (4)$$

3. Update  $U^{(k)}, U^{(k+1)}$

$$U_{ij} = \frac{1}{\sum_{i=1}^c \left( \frac{\|x_i - c_j\|}{\|x_i - c_k\|} \right)^{\frac{2}{m-1}}} \quad (5)$$

4. If  $\|U^{(k+1)} - U^{(k)}\| < \epsilon$  then STOP; otherwise return to step 2.

$u_{ij}$  is between 0 and 1,  $c_i$  denotes the centroids of cluster I,  $d_{ij}$  is the Euclidean distance between  $i^{\text{th}}$  centroid and  $j^{\text{th}}$  data point,  $m \in [1, \infty]$  is a weighting function.

This iteration will stop when  $\max_{ij} \{|u_{ij}^{(k+1)} - u_{ij}^{(k)}|\} < \epsilon$  where  $\epsilon$  is a termination criterion between 0 and 1, whereas  $k$  denotes the iteration steps. This procedure converges to a local minimum or a saddle point of  $j_m$ .

FCM algorithm is a minimization operation method of iterative optimization, which needs to repeat the calculation of membership and update value of  $U_{ij}$  and  $V_i$ . If image data  $n$  is quite huge, it meets the problem of heavy calculation burden and problem to assign the initial clusters. Therefore IFCM is proposed [24] as a new center initialization algorithm for measuring the initial centers. The implementation of IFCM is presented in this chapter.

Caldairou et al. [25] described the membership function for calculating the centroids of clusters. The membership function indicates the degree of the elements belonging to a specific class. The same element can belong to various categories in different levels and the sum of the corresponding values of all the membership functions is 1. The element that is determined

belongs to a category which has the largest value of the membership function. This is the classification criterion used in the FCM-based algorithms. But, the algorithm is still sensitive to the initial cluster centers.

Hema Rajini et al. [24] proposed an enhanced k-means and improved kernelised FCM with improved cluster center initialization algorithm to segment the MRI brain images. The method selected the initial center used by the center initialization algorithm. This algorithm was based on maximum measure of the distance function which was found for cluster center detection process. The validity of clustering results was obtained using silhouette method and the results were compared with those of original k-means and FCM algorithms. The addition of post-processing technique to extract the tumor in MRI brain image could improve the detection of brain tumor results.

Zou Kaiqil et al. [22] proposed an IFCM algorithm for color image segmentation. It was proposed to solve the problem of heavy calculating burden and the disadvantage of clustering performance affected by initial cluster centers for FCM. The quick subtractive clustering (QSC) was used for getting initial cluster centers of the image data points. In order to reduce the computational complexity, the mapping from pixel space to Eigen vector space was used for modifying the object function. The algorithm was limited to only for the general image segmentation process and further a post-processing improvement was needed for detecting tumor in MRI images.

Yongmin Kim et al. [26] discussed a novel segmentation procedure. In this method, the segmentation played a crucial role in numerous biomedical imaging applications, assisting clinicians or medical professionals to diagnose various diseases using scientific data. It required high computational time which limited its applicability.

William Sandham et al. [27] proposed a FCM segmentation of MRI brain image using neighborhood attraction with neural-network optimization. In this method, the updating process combined the classified elements and the membership functions instead of the traditional operations which rely on the data points. If the MRI image contains noise or is affected by the presence of artifacts, it can change the pixel intensities leading to improper segmentation. These problems must be properly addressed to improve the updating of membership value of the FCM algorithm.

Maoguo Gong et al. [28] explained an FCM Clustering with local information and kernel metric for image segmentation. An IFCM algorithm for image segmentation introduced a tradeoff between weighted fuzzy factor and a kernel metric. The new algorithm adaptively determined the kernel parameter by using a fast bandwidth selection rule based on the distance variance of all the data points in the collection. The weighted fuzzy factor depended both on the distance of all the neighboring pixels and their gray-level difference. By using this factor, the new algorithm could accurately estimate the damping extent of the neighboring pixels.

Ref. [29] addressed the FCM algorithm for GBM brain tumor segmentation. They used T1-weighted, T2-weighted, and Proton Density(PD)-weighted MRI with a vectorial FCM to segment the pathological brain into white matter, gray matter, cerebral fluid, tumor, and edema. Although the FCM algorithm was simple, fast and unsupervised, it could not segment the

tumor and edema accurately because of the intensities of the overlapping tissues. The FCM was very sensitive to noise and initialization values and it was validated and tested for limited cases.

Zulaikha Beevi et al. [30] presented a robust and efficient approach for the segmentation of noisy medical images. The proposed approach utilized the histogram-based FCM clustering algorithm for the segmentation of MRI brain images and the cluster density was focused. The heavy calculating burden was the drawback of this method.

In all the methods applied to the brain tumor segmentation, the partitioning of the data was carried out through a membership function at each iterative process. In the iterative process, the samples of the same groups were more similar to one another than the samples belonging to different groups. The major drawback of the FCM is that it is sensitive to the initialization problem due to noise, initial centers of clusters, and different sizes of tumor. The computational time is high for executing the segmentation process.

In all the above studies fuzzy C-means method and its steps for segmenting and detecting tumor of the MRI brain images are discussed.

#### *1.4.2. Image segmentation using region growing (RG) method*

The region growing methodology and recent related work of region growing are described here.

RG is a simple image segmentation method based on the seeds of region [31]. It is also classified as a pixel-based image segmentation method since it involves the selection of initial seed points. This approach to segmentation examines the neighboring pixels of initial “seed points” and determines whether the pixel neighbors should be added to the region or not based on certain conditions. In a normal region growing technique, the neighbor pixels are examined by using only the “intensity” constraint. A threshold level for intensity value is set and those neighbor pixels that satisfy this threshold is selected for the region growing. The processing steps are

- Select the initial seed point
- Append the neighboring pixels—intensity threshold
- Check threshold of the neighboring pixel
- Thresholds satisfy-selected for growing the region.
- Process is iterated to end of all regions.

Ref. [32] explained an automatic approach for segmenting the MRI images. The segmentation problem was formulated as a problem in region growing. In particular, the method started locally by searching for a seed region of the left atrium from an MRI slice. A global constraint was imposed by applying a shape prior to the representation of left atrium by Zernike moments. The planning and evaluation procedures of left atrium ablation were commonly based on the segmentation of the left atrium which was a challenging task due to large anatomical variations.



Yunliang Cai et al. [33] carried out detecting, grouping, and structure inference for invariant repetitive patterns in the images. Repetitive patterns are products of repetitive structures, repetitive reflections, or color patterns. The segmentation algorithm proposed in this paper followed the classical region growing image segmentation scheme. It utilized a mean-shift-like dynamic process to group the local image patches into clusters. It exploited a continuous joint alignment to match similar patches and refined the subspace grouping. The result of higher level grouping of image patterns could be used to infer the geometry of objects and estimate the general layout of a crowded scene.

Shafaf Ibrahim et al. [31] presented a comparison of segmentation algorithm performances between three techniques of seed-based region growing (SBRG), adaptive network-based fuzzy inference system (ANFIS), and FCM paradigms. All the three methods were found to be promising for segmentation of light abnormalities. Nevertheless, the segmentation performances of dark abnormalities were observed to produce moderate significances of correlation values in all conditions. These resulted in the segmentation of dark abnormalities becoming not as good as the segmentation in light abnormalities.

Nigri Happ et al. [34] presented a region growing segmentation algorithm for parallel version of graphics processing units. This method widely used by the geographic object-based image analysis. Initially, all the image pixels were considered as seeds or primitive segments. The fine-grained parallel threads assigned to the individual pixels merged the adjacent pixels iteratively and ensured that the increase in heterogeneity was minimized. The accuracy of the segmentation is low based on this approach.

Aman Chandra Kaushik et al. [35] proposed a content-based active contour method (CBAC) using both intensity and texture information present within the active contour. It also used a Gray-Level Co-occurrence Matrix (GLCM) to define texture space for tumor segmentation in MATLAB. The region growing method was used for segmenting ROI and edge detection by utilizing the boundary segmentation. The main drawback of this method was under segmentation and over segmentation.

Bhoi and Meher [36] presented a method for the removal of Gaussian noise for MRI images. It performed well in terms of peak signal to noise ratio (PSNR) over many well-known spatial and wavelet domain methods. The method also retained the edges beside the region growing methods for segmenting the MRI brain images.

Bhandarkar and Nammalwar [37] investigated the application of a hierarchical self-organizing map (HSOM) to the problem of segmentation of multispectral MRI images. The HSOM was composed of several layers of self-organizing maps (SOMs) organized in a pyramidal fashion. SOMs were used for the segmentation of multispectral MRI images, but the results often suffer from under segmentation or over segmentation.

James Tilton [38] described an approach for producing high quality hierarchically related image segmentation method. The hierarchically related image segmentations were at different levels in which the less-detailed segmentations could be produced from specific region merging algorithm. The region merging based hierarchical segmentation (HSEG) was presented, along with its recursive hierarchical segmentation (RHSEG). It was applied for exploiting the

information content from the segmentation hierarchy based on changes in the region features. The seed point selection in the hierarchical segmentation as well as recursive hierarchical segmentation was still challenging in this approach.

Jabbar et al. [39] explained the major role of the image segmentation in biomedical imaging applications such as the enumeration of tissue volume diagnosis, confinement of pathology analysis of anatomical structure, treatment planning, partial volume improvement of practical imaging data, and computer incorporated surgery.

Jaya et al. [40] explained that the tumor types and classification of the tumor could straightforwardly wipe out all the fit brain cells. They explained the detail survey about the brain tumor and explained the effect of brain tumor. They also explained the brain tumor strong cells by crowding further parts of the brain and bringing about inflammation, brain swelling, and pressure inside the skull.

Jue Wu et al. [41] proposed a framework for multi-object segmentation of deep brain structures, which have significant shape variations and relatively small sizes in medical brain images. The method suggested a template-based framework, which fused the information of edge features, region statistics, and inter-structure constraints to detect and locate all the targeted brain structures. The multi-object template was organized in the form of a hierarchical Markov dependence tree. It was applicable for multi-object segmentation of deep brain structures (caudate nucleus, putamen, and thalamus) in the MRI brain images.

Kekre et al. [42] presented a vector quantization segmentation method to detect cancerous mass from MRI images. In order to increase the radiologist's diagnostic performance, a computer-aided diagnosis scheme was developed to improve the detection of primary signatures of these diseased masses and micro-classifications.

Corso et al. [43] presented a method for automatic segmentation of heterogeneous image data where the Bayesian formulation was included to incorporate the soft model assignments for calculating affinities.

Liao et al. [44] proposed a fast spatially constrained kernel clustering algorithm for segmentation which corrected the intensity in homogeneities for the MRI brain images. A filter for random noise removal was adapted to reduce the noise in MRI images. This parametric filter, named Non-local means, was highly dependent on the setting of its parameters.

Anand et al. [45] discussed a wavelet-based bilateral filtering scheme for noise reduction in magnetic resonance images. In this method, an algorithm was proposed for 2D image de-noising and segmentation using redundant discrete wavelet transform. A two-stage de-noising algorithm was presented for the image segmentation. The importance of noise removal for the MRI was explained.

Cybenko et al. [46] explained the benefit of neural networks that lies in the subsequent theoretical facets. First, the neural networks are data-driven self-adaptive methods in which they can fine-tune themselves to the data exclusive of any clear specification of functional or distributional form for the unique model. Second, they are universal functional approximations in which neural networks can approximate the functions with random accuracy. It explained the importance of classification process in brain tumor detection.

Wan et al. [47] reported that the neural networks were non-linear models, which made them stretchable in the model and define real world intricate relationships. The neural networks that are able to approximate the subsequent probabilities, offer the basis for setting up classification rules and statistical analysis.

Pratt et al. [48] explained the RG method that involved the selection of initial seed points. It examined the neighboring pixels as initial “seed points” and determined whether the pixel neighbors should be added to the region or not based on certain conditions. The importance of the seed point selection was also explained.

In all the above methods, region growing methods and its steps for segmenting and detecting tumor in dark abnormalities of the MRI brain images are discussed.

#### *1.4.3. Image segmentation using genetic algorithm-based method*

The genetic algorithm (GA) description and some of the recent researches for segmentation based on genetic methodologies are as follows:

The genetic algorithm (GA) is a population-based stochastic search procedure to find exact solutions to the optimization and search problems. The GA creates a sequence of populations for each successive generation by using a selection mechanism and the operators such as selection, crossover, and mutation.

The GA explains an objective function or fitness function value used to evaluate the ability of each chromosome for providing a satisfactory solution to the problem ([49]). The selection procedure, modeled on nature’s survival-of-the-fittest mechanism, ensures that the fitter chromosomes have a greater number of off springs in the subsequent generations. For the crossover, two chromosomes are randomly chosen from the population set. After crossover mutation is the second operator which is used for randomizing the search. Mutation alters the content of the chromosomes at a randomly selected position of the chromosome, after determining whether the chromosome satisfies the mutation probability.

Mahindra Pratap Panigrahy et al. [50] proposed a face recognition method using GA and neural networks. The pattern recognition or face recognition problems deal with the combinations of GA with BPNN. The pattern recognition is a problem in time complexity because it requires a careful investigation about different type of patterns for huge database.

Elnomery Zanaty and Ahmed Ghiduk [51] presented a hybridization of the GA and seed region growing to produce medical image segmentation. A new fitness function was presented for generating global minima of the objective function, and a chromosome representation suitable for the process of segmentation was proposed. The RG algorithm used an initial seed point to find accurate regions for each gene. The fitness function was used to evolve the population for getting the best region for each gene. The chromosomes were updated by applying the operators of GA to evolve segmentation results. The time complexity was a drawback of this method, because the calculations of fitness function for each population set took time.

Wang et al. [52] presented a combined GA with clustering FCM method. The parameters in the GA were adjusted adaptively according to the value and the varying velocity of individual fitness to increase the genetic algorithm’s adaptability. The constraint based on the second

order derivative of histogram was introduced into genetic algorithm to reduce the searching scope and increase the efficiency of calculation. The combined GA with FCM clustering method suffered due to over segmentation problem.

Halder et al. [53] described a GA-based approach for gray-scale image segmentation that segmented the image into various constituent parts automatically. They used FCM clustering to help in generating the population of GA to automatically segment the image. The FCM algorithm assigned pixels to each category by using fuzzy membership function and then adjusted the values of the cluster centers encoded in the chromosome, replacing them by the mean points of the respective clusters. The main disadvantage of the hybridization methods was the difficulty in searching the proper number of classes in case of FCM which lacked the number of clusters.

Mohamad Awad et al. [54] discussed a multi-component image segmentation using a genetic algorithm and artificial neural network. Several methods were developed to segment the multi-component images. The multi component image segmentation method was developed using a non-parametric unsupervised artificial neural network called Kohonen's Self-Organizing Map (SOM) and hybrid genetic algorithm (HGA). The SOM was used to detect the main features of the image; then, HGA is used to cluster the image into homogeneous regions without any prior knowledge. These were performed on different satellite images to confirm the efficiency and robustness of the SOM-HGA method compared with the iterative self-organizing DATA analysis technique (ISODATA).

Peter Angeline et al. [29] stated an evolutionary algorithm that constructed recurrent neural networks. The GA and evolutionary programming are population-based search method that has shown promise in such complex tasks. The standard methods to induct both the structure and weight values of recurrent neural networks have assigned an assumed class of architectures to every task. This paper argued that the GA were inappropriate for the network acquisition and described an evolutionary program that simultaneously acquired both the structure and weights for the recurrent networks.

Insung Jung et al. [55] described a pattern classification of back-propagation algorithm using exclusive connecting network. The objective was to design a pattern classification model for decision support system based on the BP algorithm. The standard BPNN model connected each node from input to output layers. Time complexity of the algorithm was high and the error rate was small when the training was performed.

Amiya Halder et al. [56] proposed an unsupervised dynamic image segmentation using fuzzy Hopfield neural network with genetic algorithm. The genetic algorithm-based segmentation method could automatically segment the gray-scale images. This method mainly explained the spatial unsupervised gray-scale image segmentation that divided an image into regions. The aim of this algorithm was to produce a precise segmentation of images using intensity information along with neighborhood relationships. Fuzzy Hopfield Neural Network (FHNN) clustering helps to generate the population of genetic algorithm and it automatically segments the images with good quality.

Maulik [57] presented a detailed survey of the applications of GAs to medical image segmentation. The main challenges and issues in integrating GA for solving the optimization

problems in medical image segmentation were presented. The choices of the different genetic operators as well as the termination criteria were discussed. The important issues in GA and the expert knowledge, integration with local search algorithms were also discussed.

David Montana et al. [58] proposed training feed forward neural networks using genetic algorithms. The multilayered feed forward neural networks possess a number of properties which make them particularly suited to complex pattern classification problems. The genetic algorithms are a class of optimization procedures which are good at exploring a large and complex space in an intelligent way to find the values close to the global optimum. Hence, they are well suited to the problem of training feed forward networks.

### 1.5. Results and discussion

This section describes some of the experimental results of the proposed GFSMRG with BPNN technique using the MRI brain images with and without tumor. The preprocessed image and histogram generated image are shown in **Figure 12**.

### 1.6. Conclusion

MRI using segmentation method is an important diagnostic tool for the prediction of brain tumors. This chapter explains about the different segmentation methodologies for brain tumor segmentation. With a sound mechanism and clear imaging of soft tissues, the diagnosis of a patient can be scientific and rational segmentation can do with new artificial methodologies. It enables the doctors to grasp the exact progression of the disease state, which would help to make a decision about the appropriate treatment, surgery and following-up for a series of disease control measures. The computer-aided and automated segmentation tool and its analysis has reduced the workload of doctors and improved the diagnostic accuracy of the paramedical analysis.

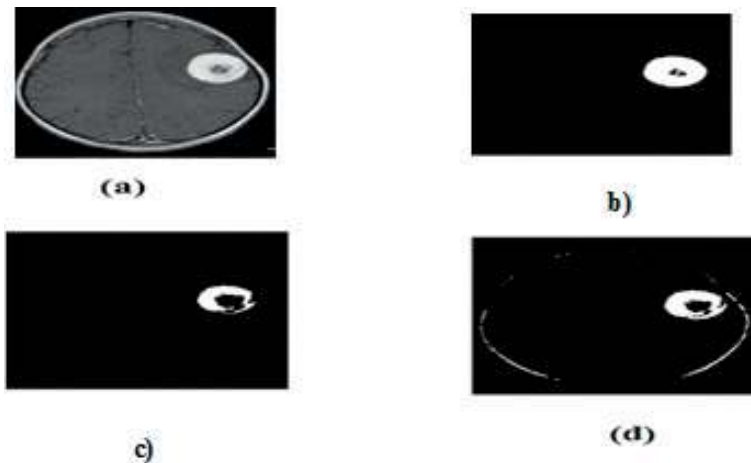


**Figure 12.** (a) Input image, (b) FCM [21], (c) RG (Shafaf [31]), and (d) GA with fuzzy ([59]).

## Author details

Kavitha Angamuthu Rajasekaran\* and Chellamuthu Chinna Gounder

\*Address all correspondence to: arkavithabalaji@gmail.com

Anna University, Chennai, Tamil Nadu, India

## References

- [1] Falk T, Shatkey H, Chan WY. Breast Cancer Prognosis via Gaussian Mixture regression. Proceedings of Canadian Conference on Electrical and Computer Eng. (CCECE '06). 2006;**64**(1):987-990
- [2] Fan Y, Rao H, Giannetta J, Hurt H, Wang J, Davatzikos C, Shen D. Diagnosis of brain abnormality using both structural and functional MR images. Conference on Proceedings of IEEE Engineering Medical and Biology Society. 2006;**11**(8):1044-1047
- [3] Gonzalez RC. Digital Image Processing. Peking: Publishing House of Electronics Industry; 2003
- [4] Shen D, Herskovits E, Davatzikos C. An adaptative-focus statistical shape model for segmentation and shape modeling of 3D brain structures. IEEE Transaction on Medical Imaging. 2001;**3**(4):257-270
- [5] Li S, Tan M. Gene selection and tissue classification based on support vector machine and genetic algorithm. IEEE International Conference on Bio-Informatics and Biomedical Engineering. 2007;**7**(4):244-259
- [6] Stark DD, Bradley WG. Magnetic Resonance Imaging. 3rd ed. Mosby; 1999. pp. 1321-1254
- [7] Steen RG. Edema and tumor perfusion: Characterization by quantitative HMR imaging. American Journal of Radiology. 1992;**158**:259-264
- [8] Huang JY, Liang XY. The Basic Principles of Medical Imaging. Beijing: Electronic Industry Press; 2009
- [9] Zhan Y, Tan GX. Medical Imaging Diagnostic Lab Manual. Wuhan Hubei Science and Technology Press; 2009
- [10] Yang ZH, Feng F, Wang XY. MRI guide-check specification, clinical strategies and application of new technologies. Beijing: People's Medical Publishing House. 2010;**5**(2):34-49
- [11] Armstrong TS, Cohen MZ, Weinbrg J, Gilbert MR. Imaging techniques in neuro oncology. Seminars in Oncology Nursing. 2004;**20**(4):231-239
- [12] Jacobs MA, Ibrahim TS, Ouwerkerk R. MR imaging: Brief overview and emerging applications. Radio Graphics. 2007;**27**(4):1213-1229

- [13] Haacke M, Brown R, Thompson M, Venkatesan R. *Magnetic Resonance Imaging: Physical Principles and Sequence Design*. New York: Wiley-Liss; 1999
- [14] Bushberg J, Seibert A, Leidholdt E, Boone J. *Essential Physics of Medical Imaging*. Philadelphia: Lippincott Williams & Wilkins; 2002;**10**(2):1335-1347
- [15] Cruickshank G. *Tumours of the brain surgery*. Oxford. 2004;**22**(3):69-72
- [16] [www.usa.siemens.com/healthcare](http://www.usa.siemens.com/healthcare), 2012
- [17] Wu EH, Feng GS, Bai RJ. *Medical imaging (the 6th edition)*. Beijing: People's Medical Publishing House, vol. 40, no. 9, pp. 156-163
- [18] Tsuchiya K, Mizutani Y, Hachiya J. Preliminary evaluation of fluid attenuated inversion-recovery MR in the diagnosis of intracranial tumors. *American Journal of Neuro radiology*. 1996;**17**(6):1081-1086
- [19] Wang CZ. *Neurosurgery*. Beijing: People's Medical Publishing House. 2002;**47**(12):456-459
- [20] Seer 2011, [www.abta.org](http://www.abta.org)
- [21] Jude Hemanth D, Selvathi D, Anitha J. Effective Fuzzy Clustering Algorithm for Abnormal MR Brain Image Segmentation. *International Advance Computing Conference*. 2009;**13**(7):609-614
- [22] Kaiqi Z, Zhiping W, Ming H. An Improved FCM algorithm for Color Image Segmentation. *The 3rd International Conference on Innovative Computing Information and Control (ICICIC'08)*. 2009;**22**(4):15-27
- [23] Pham DL, Xu CY, Prince JL. A survey of current methods in medical image segmentation. *Annual Review of Biomedical Engineering*. 2008;**2**(7):315-337
- [24] HemaRajini N, Bhavani R. Enhancing K-means and Kernelized fuzzy C-means clustering with cluster center initialization in segmenting MRI brain images. *IEEE 3rd International Conference on Electronics Computer Technology (ICECT)*. 2011;**2**(7):259-263
- [25] Caldaïrou B, Passat N, Habas PA, Studholme C, Rousseau F. A non-local fuzzy segmentation method: Application to brain MRI. *Pattern Recognition*. 2011;**44**(9):1916-1927
- [26] Kim Y, Kang M, Kim J-M. Exploration of Optimal Many-Core Models for Efficient Image Segmentation. *IEEE Transactions on Image Processing*. 2013;**22**(6):1767-1777
- [27] Sandham W. 'MRI fuzzy segmentation of brain tissue using neighborhood attraction with neural-network optimization', *IEEE Transactions on Information Technology in Biomedicine*, 2005;**9**(3):67-78
- [28] Gong M, Liang Y, Shi J, Ma W, Ma J. Fuzzy C-means clustering with local information and kernel metric for image segmentation. *IEEE transactions on. Image processing*. 2013;**22**(2):573-584
- [29] Angeline PJ, Saunders GM, Pollack JB. An evolutionary algorithm that constructs recurrent neural networks. *International Journal of Computer Science*. 1995;**23**(4):88-97

- [30] Zulaikha Beevi S, Mohamed Sathik M. An effective approach for segmentation of MRI images: Combining spatial information with fuzzy C-means clustering. *European Journal of Scientific Research*. 2010;**41**(3):437-451
- [31] Ibrahim S, Khalid NEA, Manaf M. Seed-based region growing (SBRG) vs adaptive network-based inference system (ANFIS) vs fuzzy c-means (FCM): Brain abnormalities segmentation. *International Journal of Electrical and Computer Engineering*. 2010;**5**(2):94-104
- [32] Zhu L, Gao Y, Yezzi A, Tannenbaum A. Automatic Segmentation of the Left Atrium from MR Images via Variation Region Growing With a Moments-Based Shape Prior. *IEEE Transactions on Image Processing*. 2013;**22**(7):1057-1071
- [33] Cai Y, Baciuc G. Detecting, Grouping, and Structure Inference for Invariant Repetitive Patterns in Images. *IEEE Transactions on image processing*. 2013;**22**(7):2343-2355
- [34] Nigri Happ P, Queiroz Feitosa R, Bentes C, Farias R. A region growing segmentation algorithm for GPUs. *IEEE Geosciences and Remote Sensing Letters*. 2013;**10**(30):1612-1616
- [35] Kaushik AC, Sharma V. Brain tumor segmentation from MRI images and volume calculation of tumor. *International Journal of Pharmaceutical Science Invention*. 2013;**7**(2):23-26
- [36] Bhoi N, Meher S. Total variation based wavelet domain filter for image denoising. *Proc. 1st Int. Conf. on Emerging trends in engineering and technology: ICETET 08, Nagpur, India, July, G. H. Rasoni College of Engineering*. 2008;**3**(3):20-25
- [37] Bhandarkar SM, Nammalwar P. Segmentation of multispectral MR images using a hierarchical self-organizing map. *Proc. 14th IEEE Symp. On Computer based medical system. CBMS Bethesda, MD, USA: IEEE Computer Society*. 2001;**6**(6):294-299
- [38] Tilton J. Analysis of hierarchically related image segmentations. *IEEE workshop on advances in technique for analysis of remotely sensed data*. 2003;**8**(8):123-139
- [39] Jabbar NI, Mehrotra M. Application of fuzzy neural network for image tumor description. *Proceeding of World Academy of Science Engineering Technology*. 2008;**2**(8):427-429
- [40] Jaya J, Thanushkodi K, Karnan M. Tracking algorithm for de-noising of MR brain images. *IJCSNS Int. J. Comput. Sci. Network Secur*. 2009;**9**(11):262-267
- [41] Wu J, Albert CS, Chung. 'A novel framework for segmentation of deep brain structures based on Markov dependence tree', *NeuroImage*. 2009;**46**(8):1027-1036
- [42] Kekre HB, Sarode T, Raut K. Detection of tumor in MRI using vector quantization segmentation. *International Journal of Computer Application*. 2010;**4**(9):14-19
- [43] Corso JJ, Sharon E, Dube S, El-Saden S, Sinha U, Yuille A. Efficient multilevel brain tumor segmentation with integrated Bayesian model classification. *IEEE Transactions on Medical Imaging*. 2008;**27**(15):629-640
- [44] Liao L, Lin TS, Li B. MRI brain image segmentation and bias field correction based on fast spatially constrained kernel clustering approach. *Journal of Pattern Recognition Letters*. 2008;**29**(5):1580-1588



- [45] Anand CS, Sahambi JS. Wavelet domain nonlinear filtering for MRI denoising. *Magnetic Resonance Imaging*. 2010;**28**(6):842-861
- [46] Cybenko L, Fan C. Robust classification for extraction for magnetic resonance imaging. *IEEE Geoscience and Remote Sensing Letters*. 1991;**5**(2):246-250
- [47] Wan E. Neural network classification: A Bayesian interpretation. *IEEE Transactions on Neural Networks*. 1990;**1**(1):303-313
- [48] Pratt WK. *Digital Image Processing*. 4th ed. Los Altos, CA: John Wiley & Sons, Inc.; 2007
- [49] Holland JH. *Adaptation in Neural and Artificial Systems*. University of Michigan press; 1975
- [50] Panigrahy MP, Kumar N. Face recognition using genetic algorithm and neural networks. *International Journal of Computer Applications*. 2012;**55**(4):145-157
- [51] ElnomeryZanaty A, Ahmed Ghiduk S. A novel approach based on genetic algorithms and region growing for magnetic resonance image (MRI) segmentation. *ComSIS*. 2013; **10**(3):1319-1342
- [52] Wang H, Zhang BJ, Liu XZ, Luo DZ, Zhong SB. Image segmentation method based on improved genetic algorithm and fuzzy clustering. *Advanced Materials Research*. 2011;**379**(7):143-144
- [53] Halder A, Pramanik S, Karm A. Dynamic image segmentation using fuzzy CMeans based genetic algorithm. *International Journal of Computer Applications*. 2011;**28**(6):15-20
- [54] Awad M, Chehdi K, Nasri A. 'Multicomponent image segmentation using a genetic algorithm and artificial neural network', *IEEE Geoscience and Remote Sensing Letters*. 2007;**4**(4):571-575
- [55] Jung I, Wang G-N. Pattern classification of back-propagation algorithm using exclusive connecting network. *World Academy of Science, Engineering and Technology*. 2007;**36**(6): 180-184
- [56] Halder A, Pramanik S. An unsupervised dynamic image segmentation using fuzzy Hopfield neural network based genetic algorithm. *IJCSI International Journal of Computer Science*. 2012;**9**(2):525-532
- [57] Maulik U. 'Medical image segmentation using genetic algorithms', *IEEE Transactions on Information Technology in Biomedicine*. 2009;**13**(2):166-173
- [58] David Montana J, Davis L. Training feedforward neural networks using genetic algorithms. *MachineLearning*. 2008;**1**(89):762-767
- [59] Kaur A, Jindal G. Tumour detection using genetic algorithm. *International Journal of Computer Science And Technology*. 2013;**4**(1):423-427

